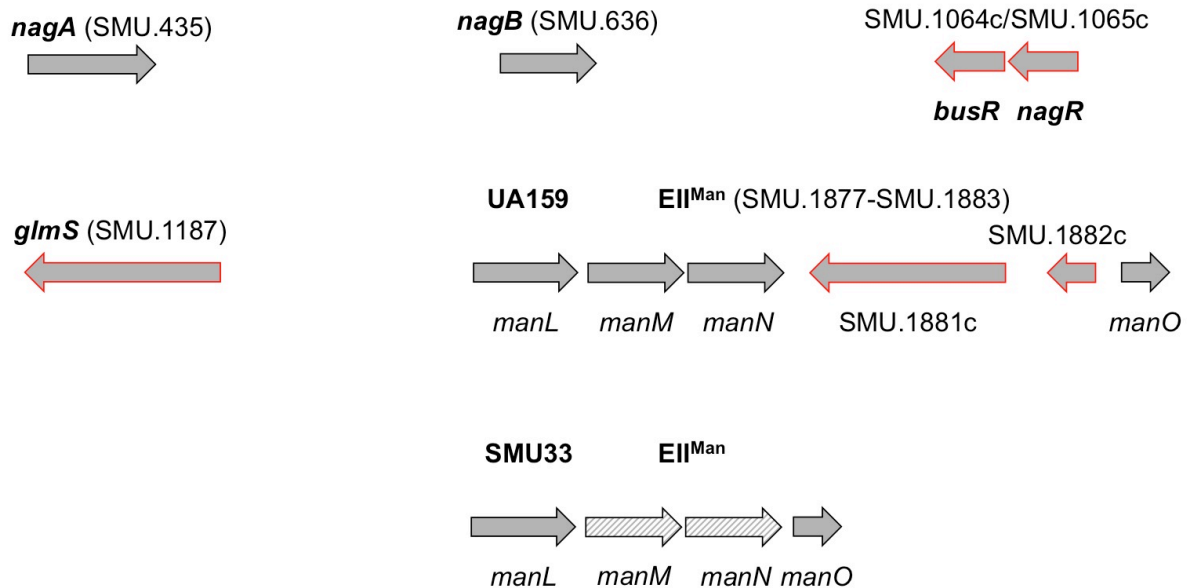


FIG S1 Schematic diagrams depicting the genomic organization of genes/operons reported in this communication (A) and features upstream of *nagA*, *nagB* and *glmS* sequences (B). (A) Each gene is represented by an arrow and all drawings are approximately in scale. Differences in the organization of the *man* operon are illustrated by displaying the arrangement of the operon within the reference strain UA159 and the clinical isolate SMU33. (B) All putative NagR-binding sites were identified bioinformatically and are available at the RegPrecise database (http://regprecise.lbl.gov/RegPrecise/regulon.jsp?regulon_id=35378). These 5 DNA sequences were used to generate a consensus sequence (top left) unique to the genome of *S. mutans* UA159, via the website of <http://weblogo.berkeley.edu/> (*Genome Research*, **14**:1188-1190, (2004)). The information regarding the promoters (-35 and -10 elements) of *nagA*, *nagB* and *glmS* was partly derived from previous publication (*PLoS ONE* **7**:e33382). +1 designates the start of the protein sequences.

A



B

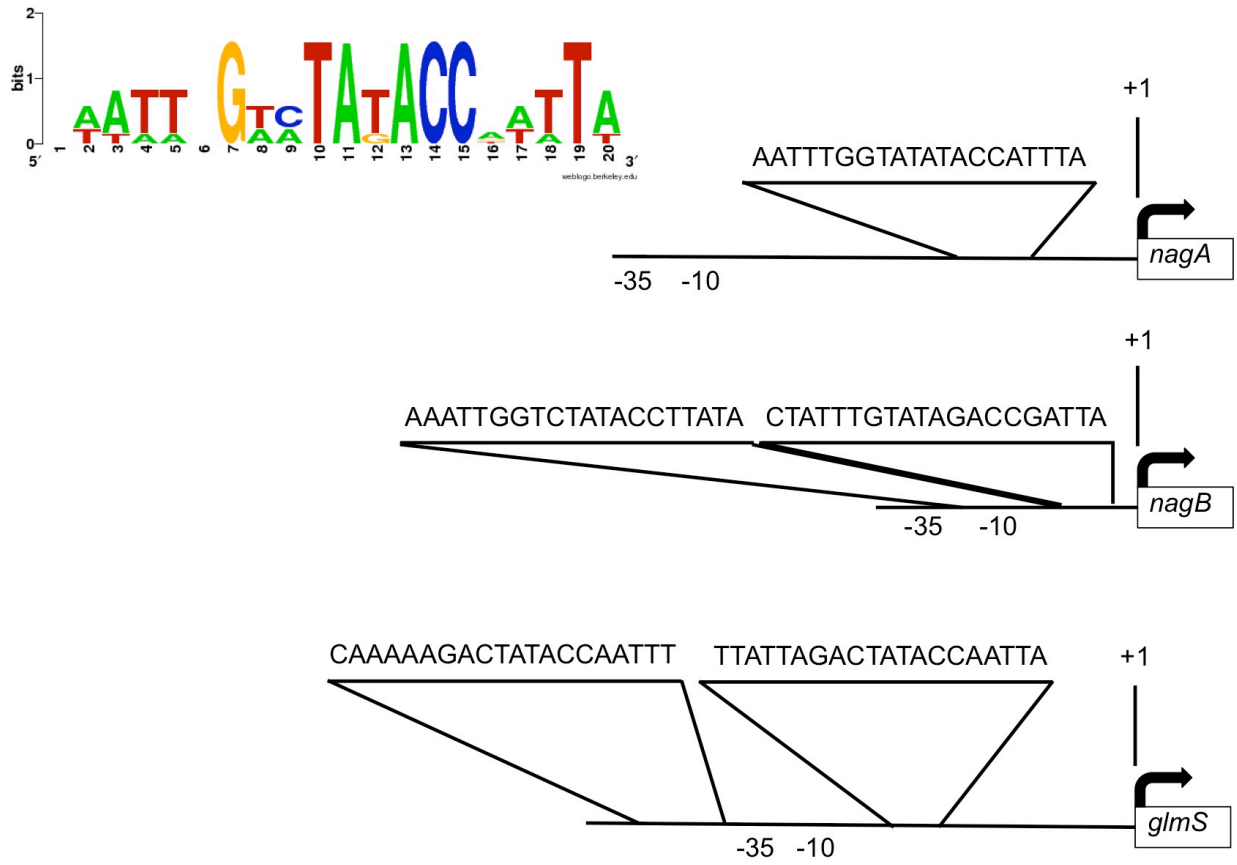


FIG S2 The levels of *manL* mRNA as determined by qRT-PCR. *S. mutans* UA159 containing the empty pBGE vector and a *manL* deletion mutant complemented with pBGE-*manL* (Δ *manL* pBGE-*manL*) were grown to mid-exponential phase in TV media supplemented with 20 mM glucose (glc), 20 mM GlcN or 20 mM GlcNAc. Cells were lysed by mechanical disruption, and RNA was extracted and used to determine *manL* mRNA levels by performed qRT-PCR.

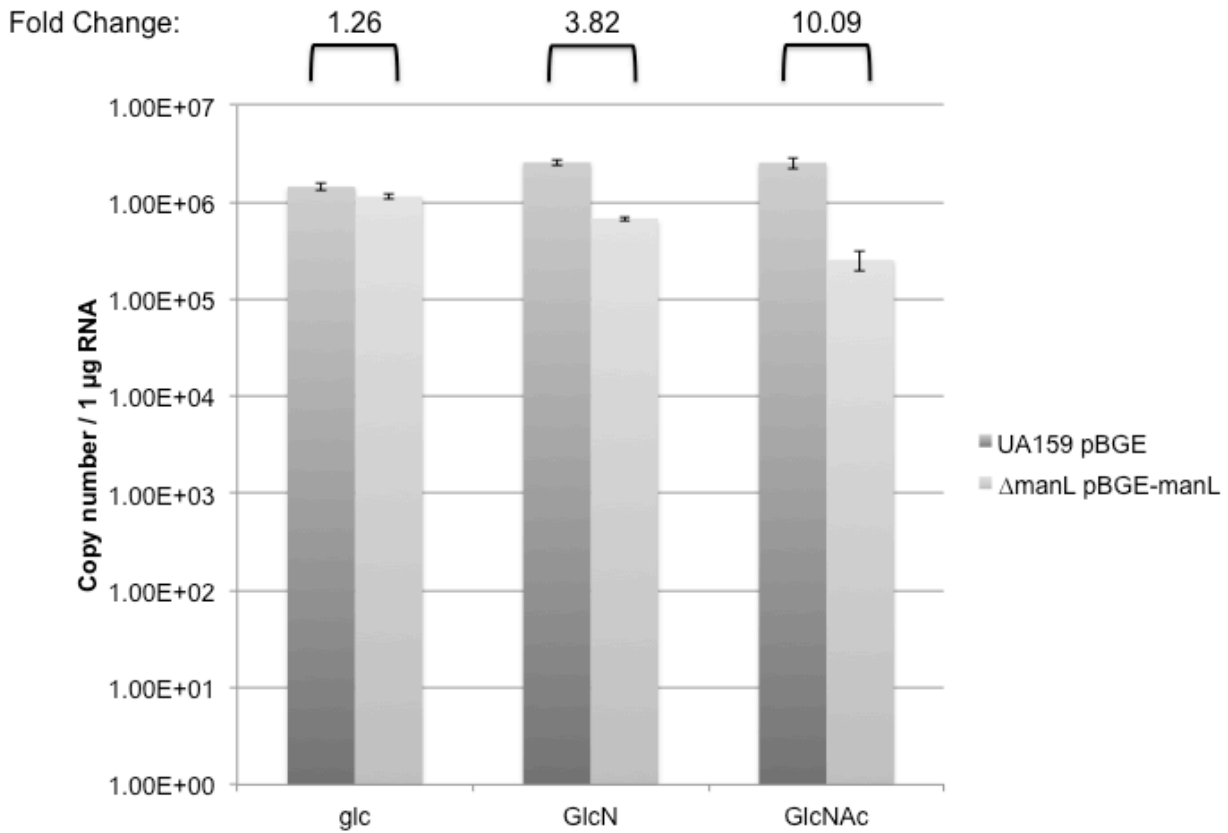


FIG S3 Immunoblotting of lysates to determine the levels of ManL. *S. mutans* UA159 containing the empty pBGE vector and a *manL* deletion mutant complemented with pBGE-*manL* (Δ manL pBGE-*manL*) were grown to mid-exponential phase in TV media supplemented with 20 mM glucose (A), 20 mM GlcN (B) or 20 mM GlcNAc (C). Cells were lysed by mechanical disruption, and equal portions of cleared lysates were separated using SDS-PAGE. Immunoblotting was performed to determine the levels of ManL using primary antibodies at previously determined optimal concentrations. Each panel represents three independent replicates of the indicated strains.

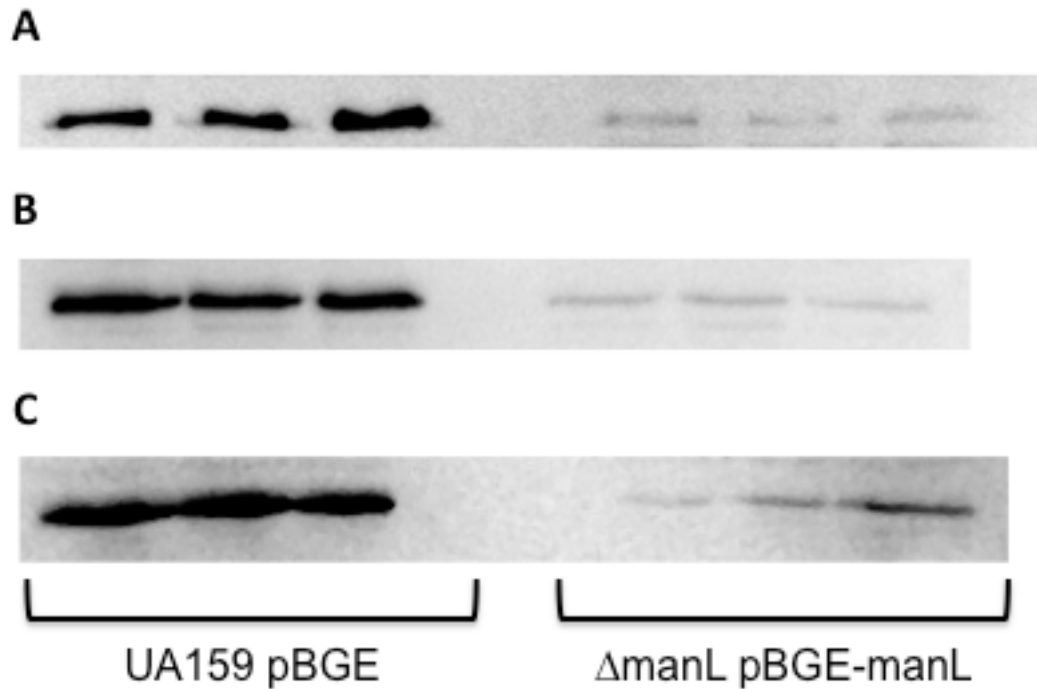
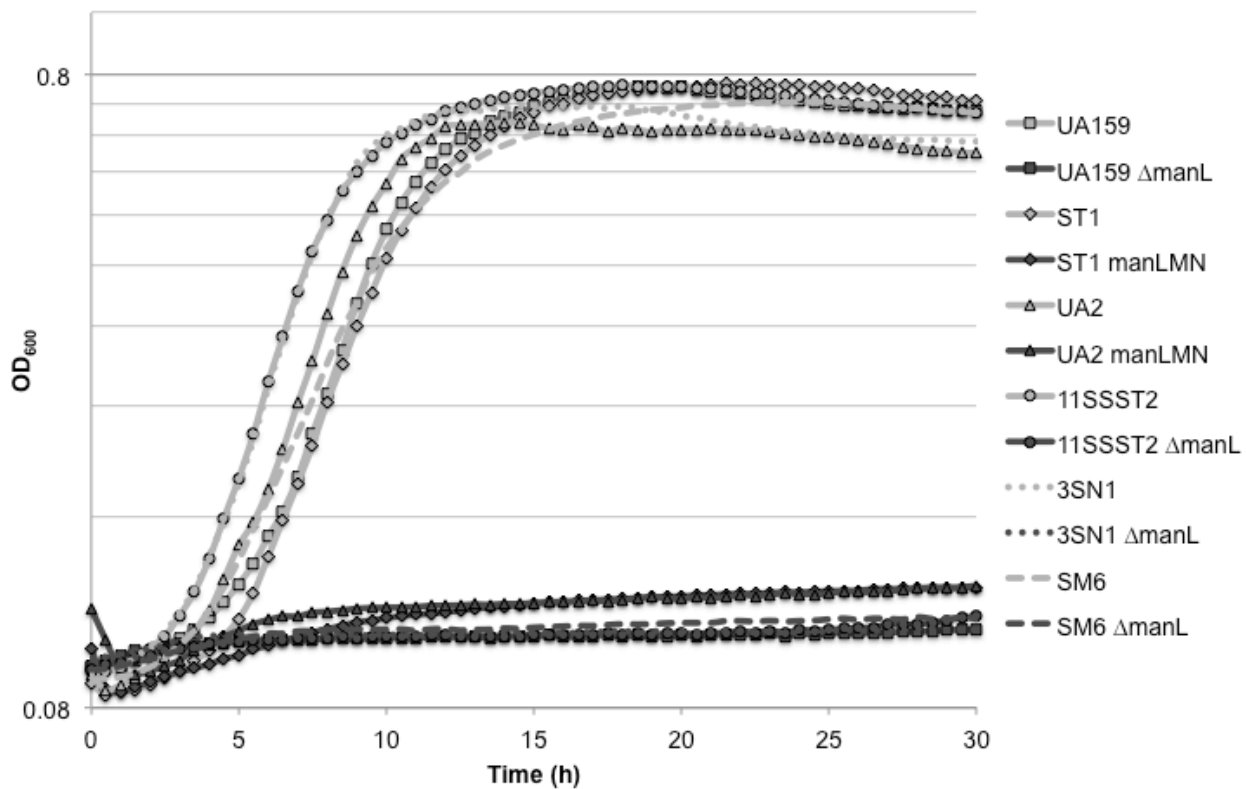
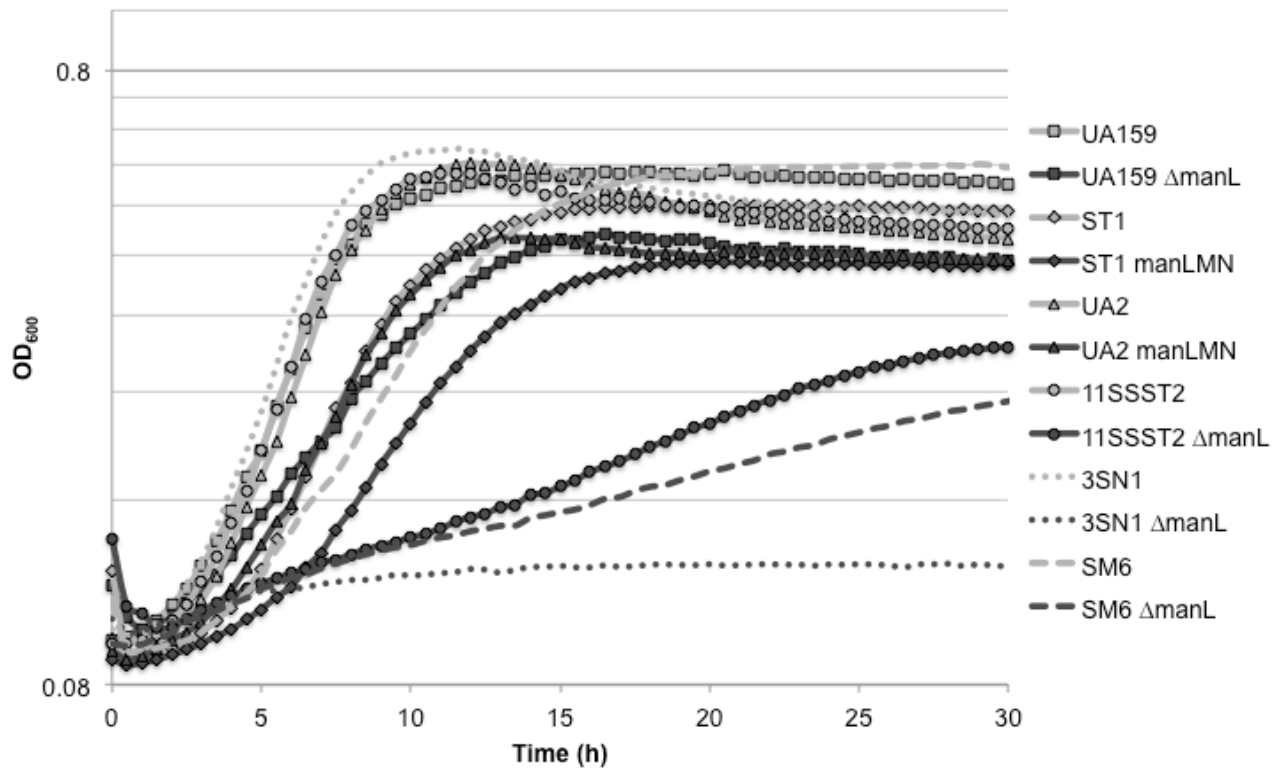
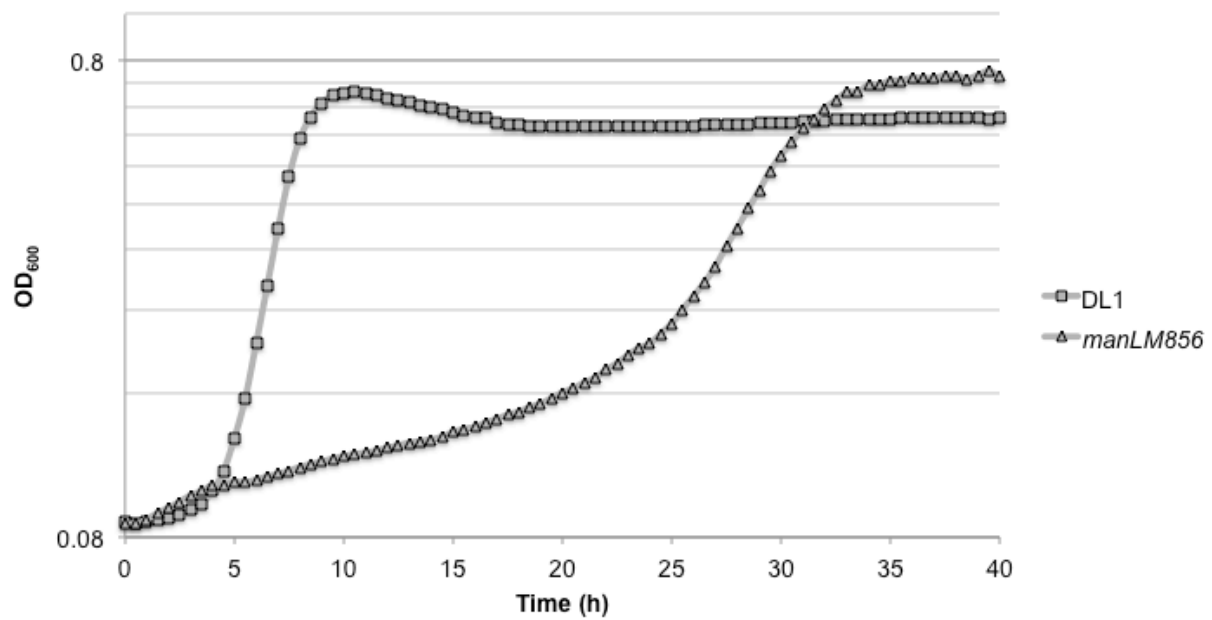


FIG S4 Growth curves of *S. mutans* UA159, five clinical isolates of *S. mutans*, *Streptococcus gordonii* DL-1 and derivatives on TV media supplemented with various carbohydrates. *S. mutans* UA159 and five clinical isolates of *S. mutans* (ST1, U2A, 11SSST2, 3SN1 and SM6) in addition to a *manL* deletion mutant of *S. mutans* UA159 (UA159 Δ manL) and *manLMN* operon deletion mutants of the clinical isolates (ST1 *manLMN*, U2A *manLMN*, 11SSST2 Δ manL, 3SN1 Δ manL and SM6 Δ manL) were grown in TV media supplemented with 20 mM GlcNAc (A) or 20 mM GlcN (B). *S. gordonii* DL-1 and a glucose/mannose EII permease deletion mutant (*manLM856*) were grown in TV media supplemented with 20 mM GlcNAc (C) or 20 mM GlcN (D).

A



B**C**

D

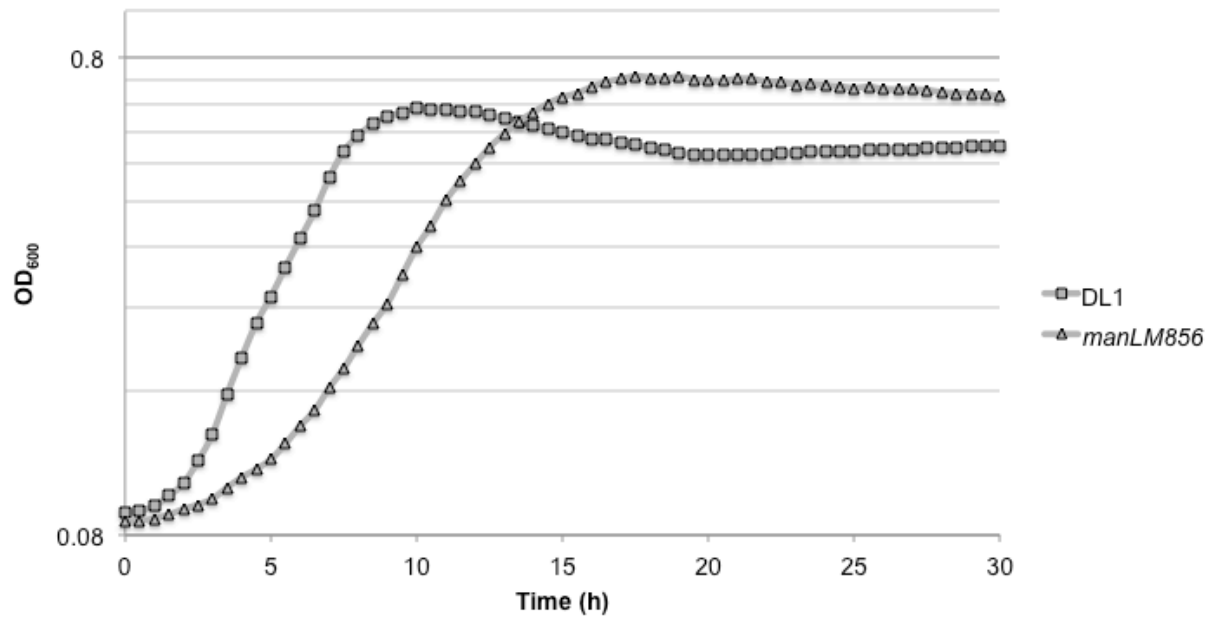
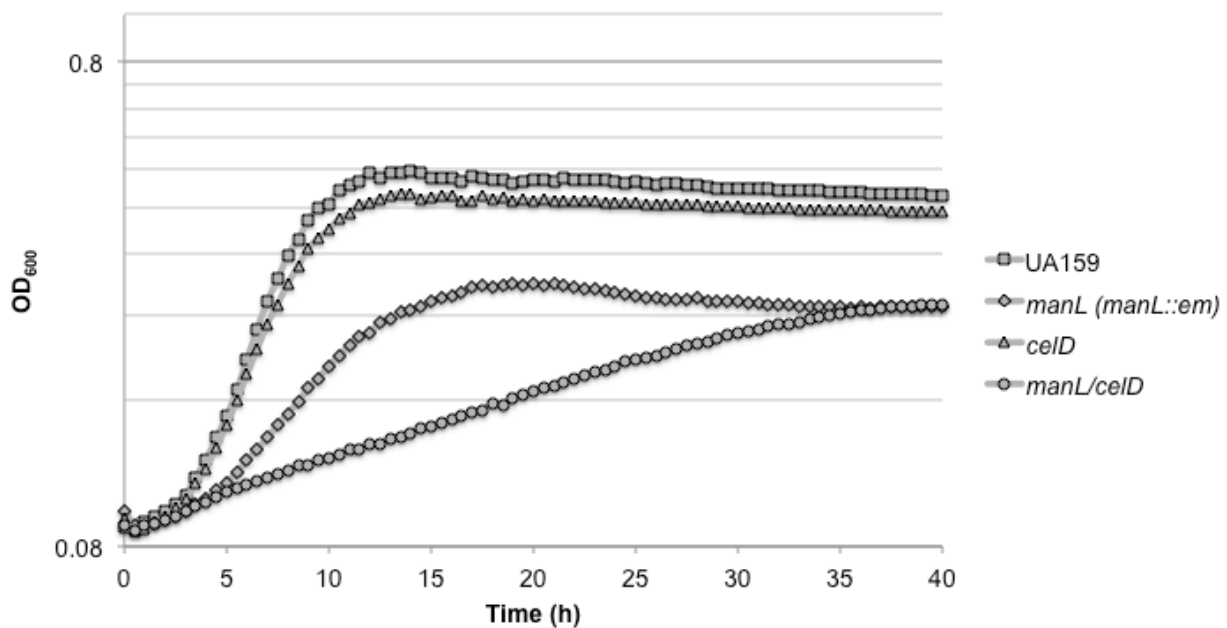


FIG S5 Growth curves of *S. mutans* UA159 and derivatives on TV media supplemented with GlcN. (A) UA159, a *manL* (*manL::em*) deletion mutant, a *celD* deletion mutant and a *manL/celD* deletion mutant (created in the *manL::em* background) were grown in TV media supplemented with 20 mM GlcN. (B) UA159, a *manL* (JAM1; *manL::km*) deletion mutant, a *fruI/fruCD/levD* deletion mutant and a *fruI/fruCD/levD/manL* deletion mutant (created in the JAM1 background) were grown in TV media supplemented with 20 mM GlcN.

A



B

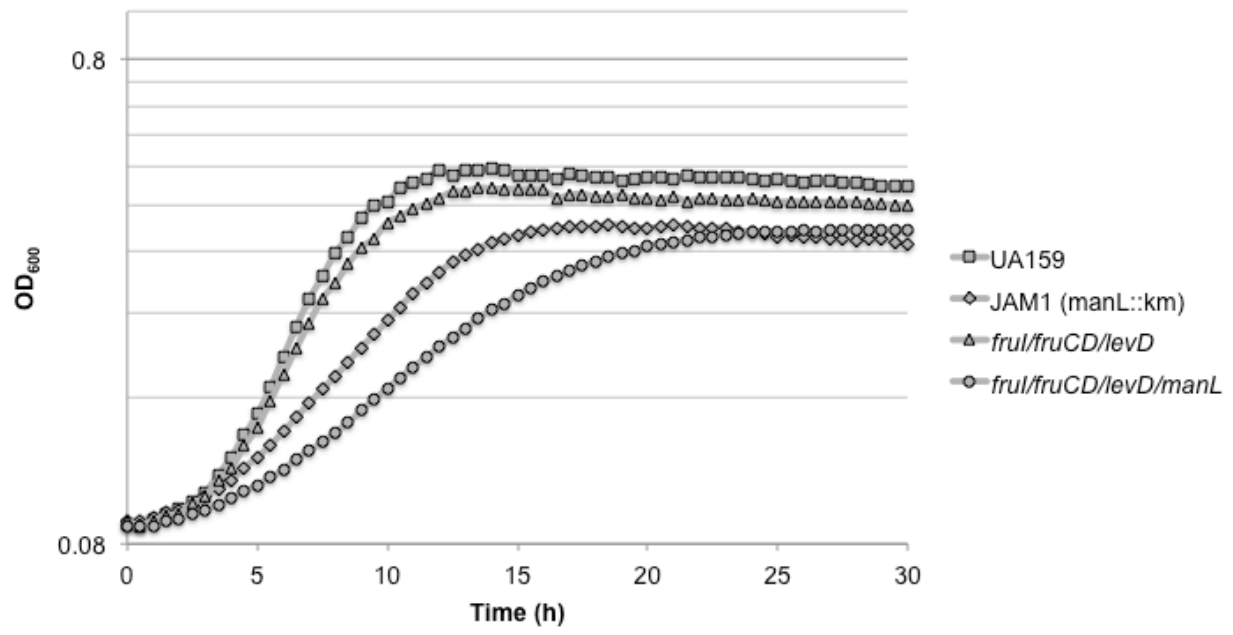
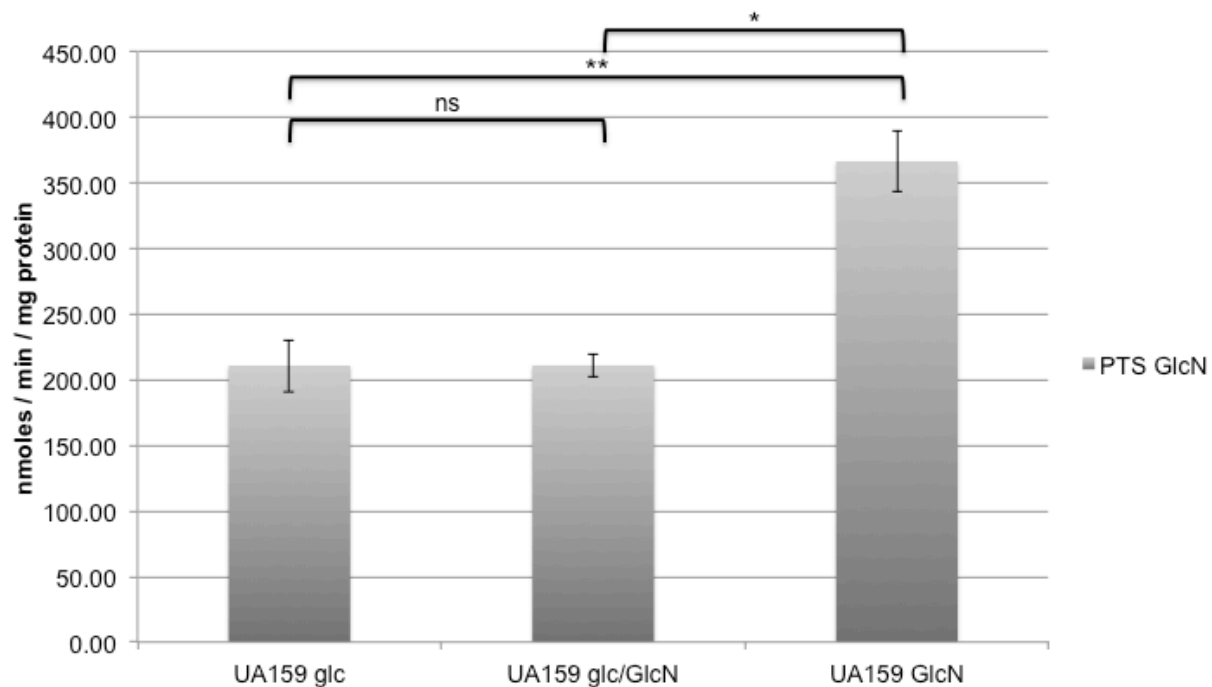
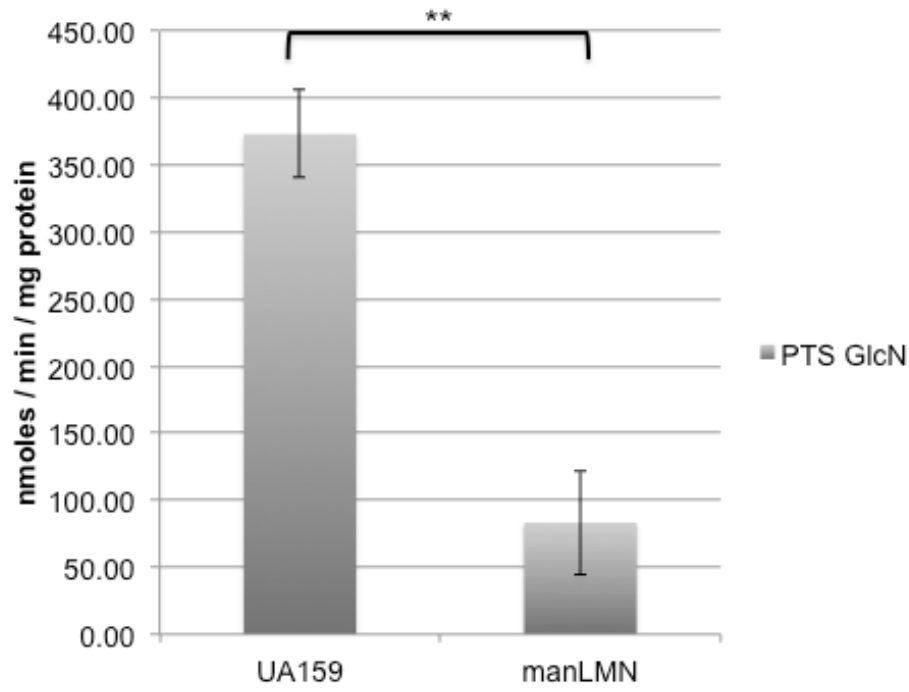


FIG S6 PTS-dependent sugar:phosphotransferase activity. *S. mutans* UA159 was grown in TV media supplemented with 20 mM glucose, 20 mM glucose and 20 mM GlcN, or 20 mM GlcN (A). In addition, *S. mutans* UA159 and a *manLMN* deletion mutant were grown in TV media supplemented with 20 mM GlcN (B) or 20 mM glucose and 20 mM GlcNAc (C). The PTS-dependent transport of GlcN (A-B) or GlcNAc (C) was determined using permeabilized cells as described in the Materials and Methods section. Each bar represents the average results of three independent experiments with error bars indicating the standard deviation. *, $P < 0.01$; **, $P < 0.001$ (by the Student *t* test). ns, not significant.

A



B



C

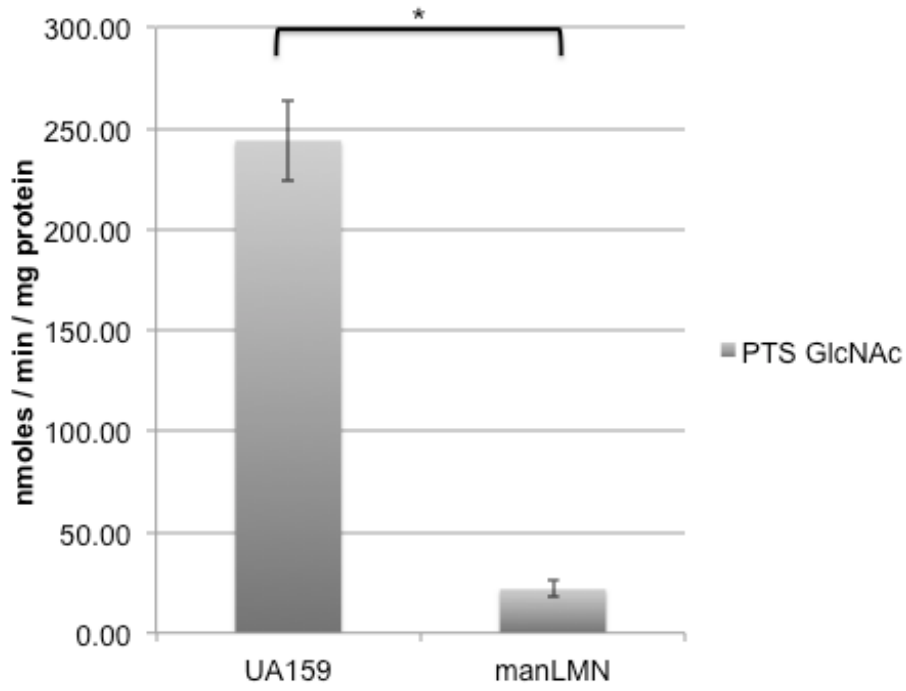
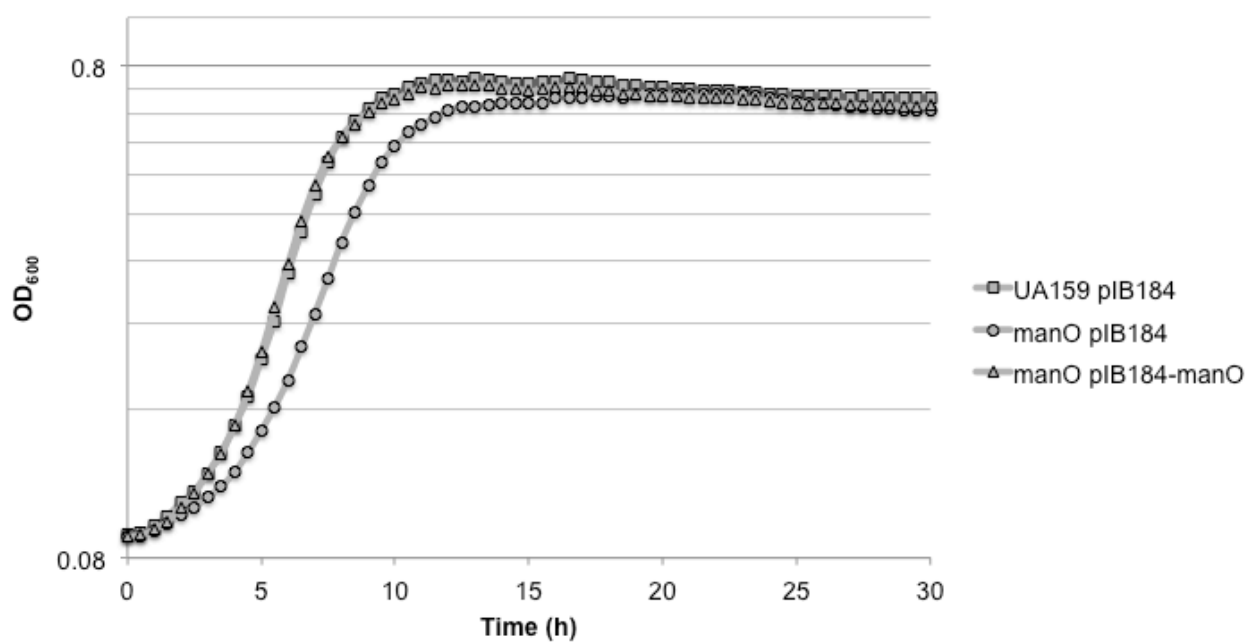


FIG S7 Growth curves of *S. mutans* UA159 containing the empty pIB184 vector (UA159 pIB184), a *manO* deletion mutant containing the empty pIB184 vector (*manO* pIB184) and a *manO* deletion mutant complemented with pIB184-*manO* (*manO* pIB184-*manO*) grown in TV media containing 3 $\mu\text{g/ml}$ of erythromycin and supplemented with 20 mM glucose (A), 20 mM GlcNAc (B) or 20 mM GlcN (C).

A



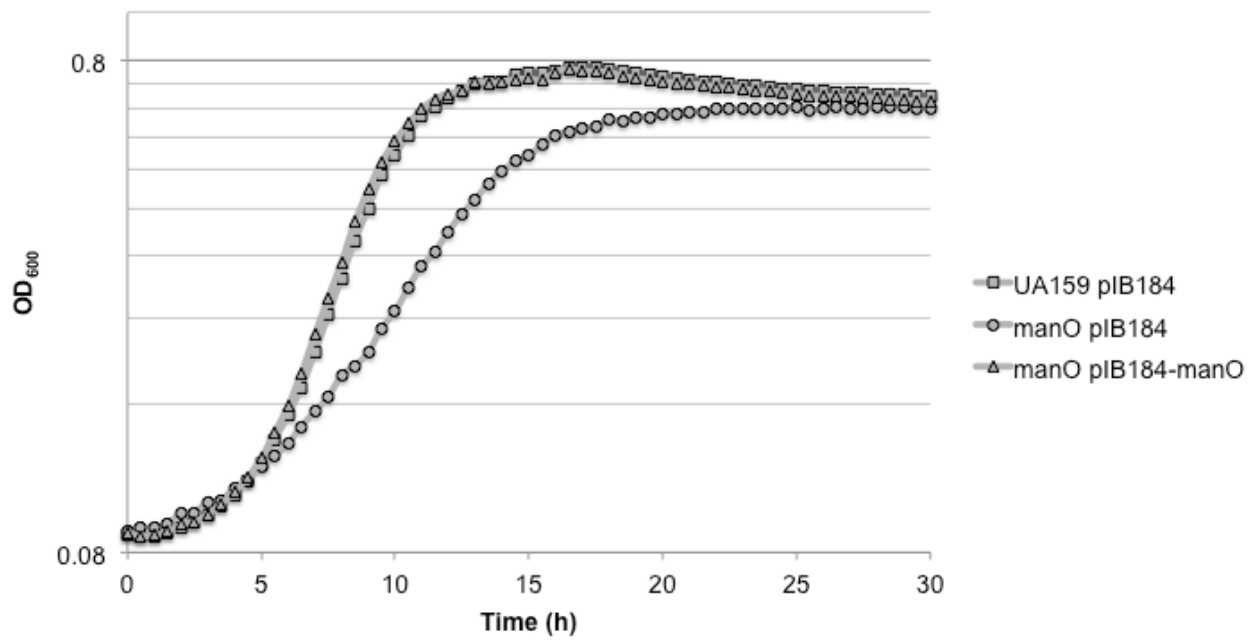
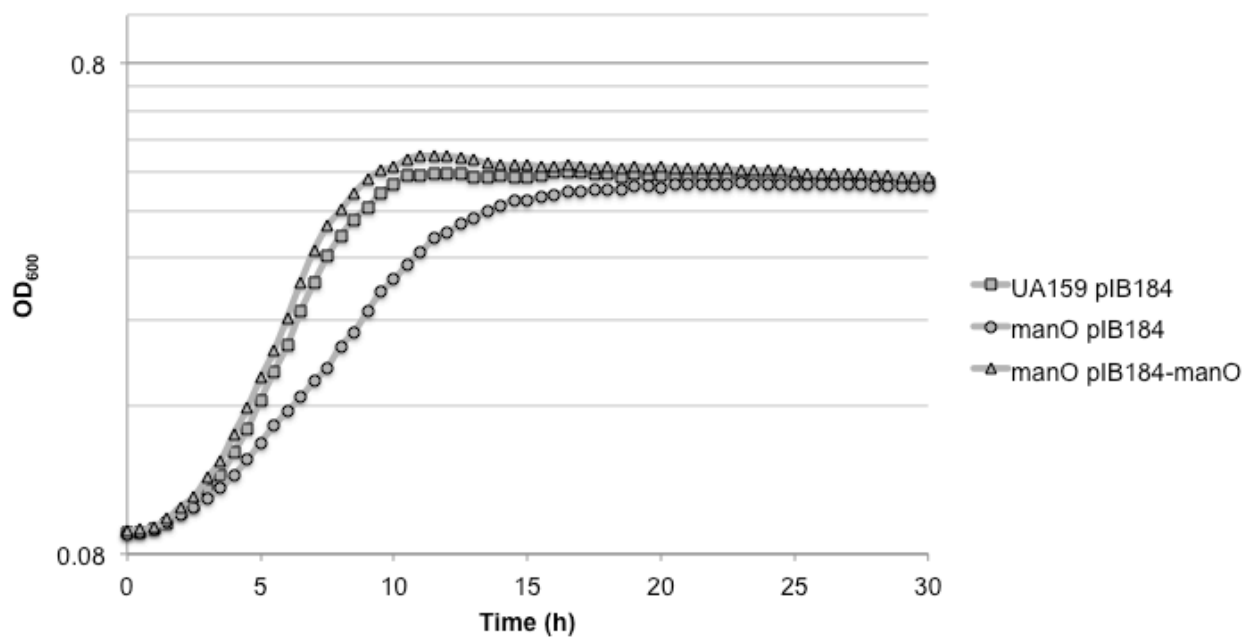
B**C**

FIG S8 Immunoblotting of lysates to determine the levels of ManL. *S. mutans* UA159 and a *manO* deletion mutant were grown in TV media supplemented with 20 mM glucose. Cells were lysed by mechanical disruption, and equal quantities of protein were separated by SDS-PAGE. The levels of ManL were determined by performing an immunoblot. Three independent biological replicates were performed for each strain.

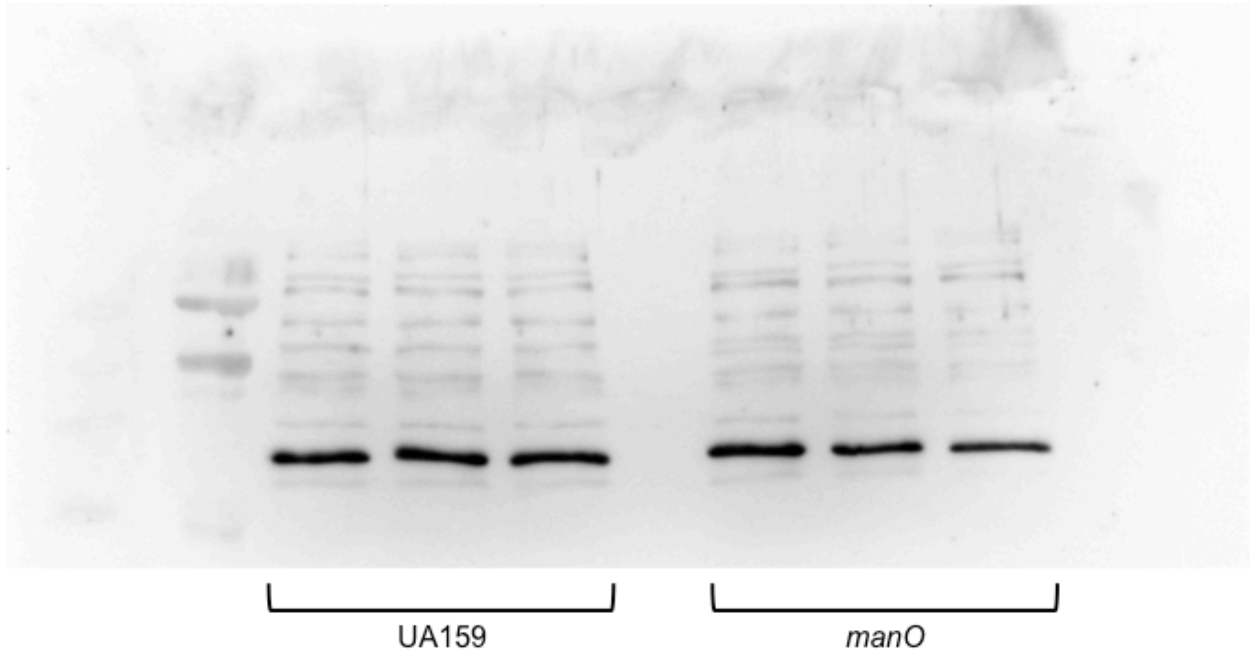


FIG S9 PTS-dependent sugar:phosphotransferase activity. *S. mutans* UA159 was grown in TV media supplemented with 20 mM glucose (UA159 glc), 20 mM glucose and 20 mM GlcNAc (UA159 glc/GlcNAc) or 20 mM GlcNAc (UA159 GlcNAc). The PTS-dependent transport of GlcNAc was determined using permeabilized cells as described in the Materials and Methods section. Each bar represents the average result of three independent experiments with error bars indicating the standard deviation. *, $P < 0.05$ (by the Student *t* test). ns, not significant.

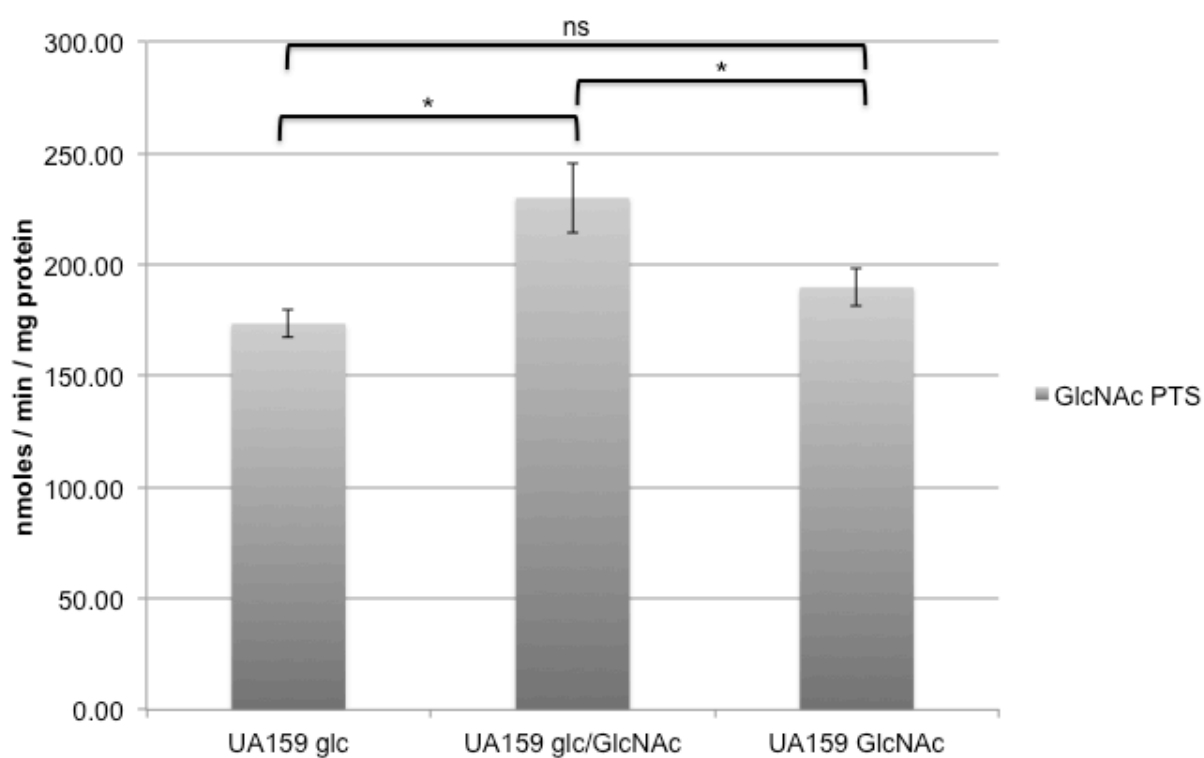


FIG S10 Immunoblot showing the levels of ManL in lysates. *S. mutans* UA159 was grown in TV media supplemented with 20 mM glucose (glc), 20 mM glucose and 20 mM GlcNAc (glc/GlcNAc), or 20 mM GlcNAc (GlcNAc). Cells were lysed by mechanical disruption, and equal quantities of protein were separated by SDS-PAGE. An immunoblot was performed to determine the levels of ManL. Three independent biological replicates of UA159 were generated for each growth condition tested.

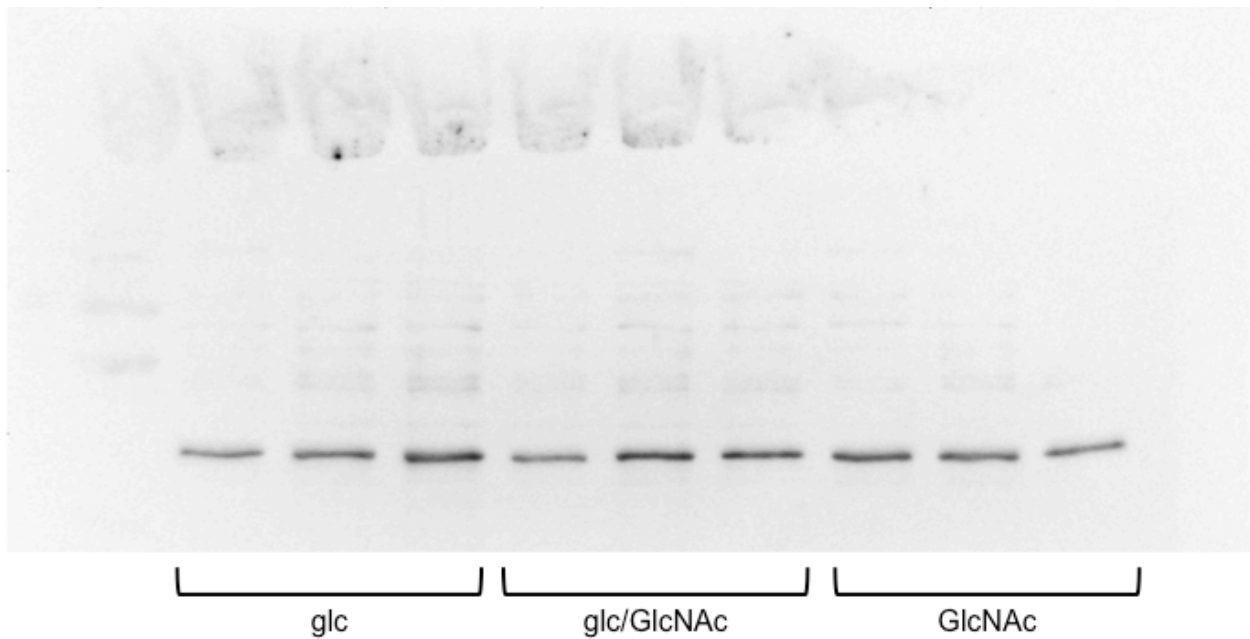
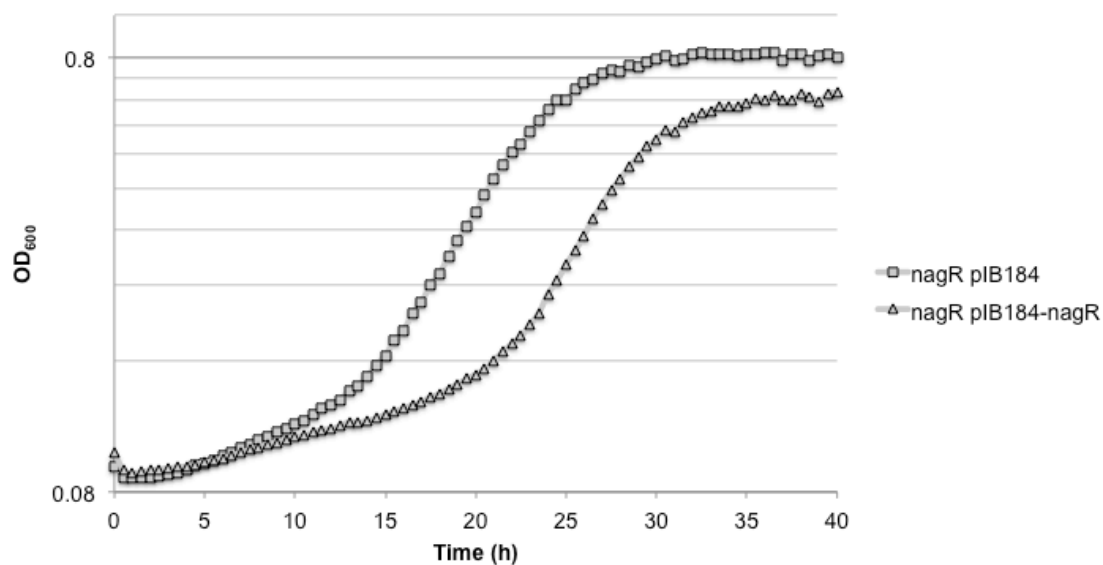


FIG S11 Growth curves of a *nagR* deletion mutant of *S. mutans* UA159 containing the empty pIB184 vector (*nagR* pIB184) and the *nagR* deletion mutant complemented with pIB184-*nagR* (*nagR* pIB184-*nagR*) grown in FMC containing 3 μ g/ml erythromycin and 20 mM GlcN (A) or 20 mM GlcNAc (B) as the sole carbon source.

A



B

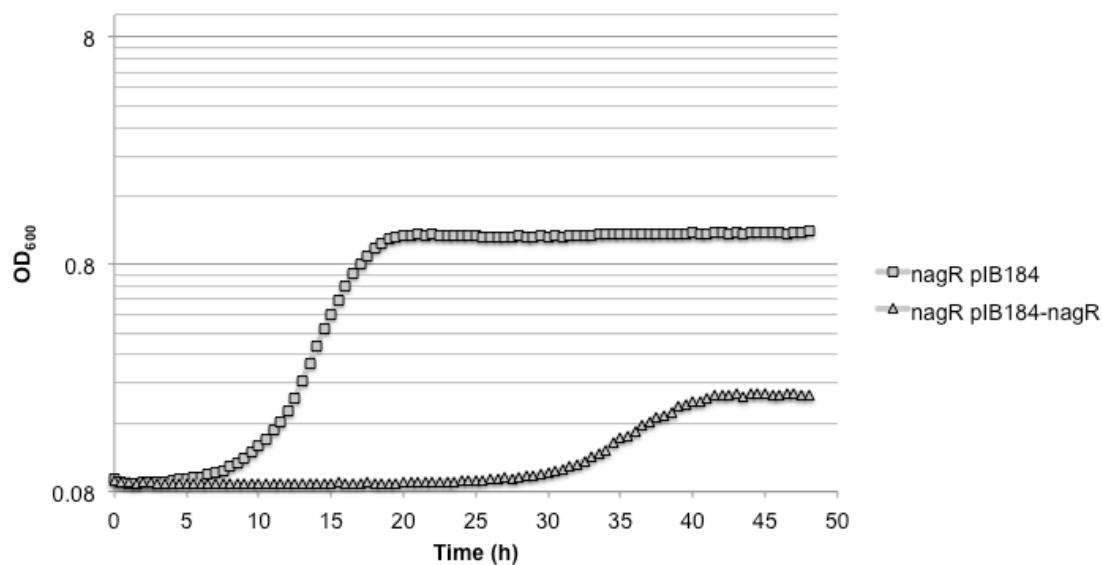


FIG S12 EMSA performed using increasing concentrations of the MBP (0-4 μ M) mixed with biotinylated DNA fragments containing regions upstream of the *nagA*, *nagB* or *glmS* gene. DNA probes and purified protein were generated as described in the Materials and Methods section. EMSA is a representative example of at least three independent experiments showing similar results.

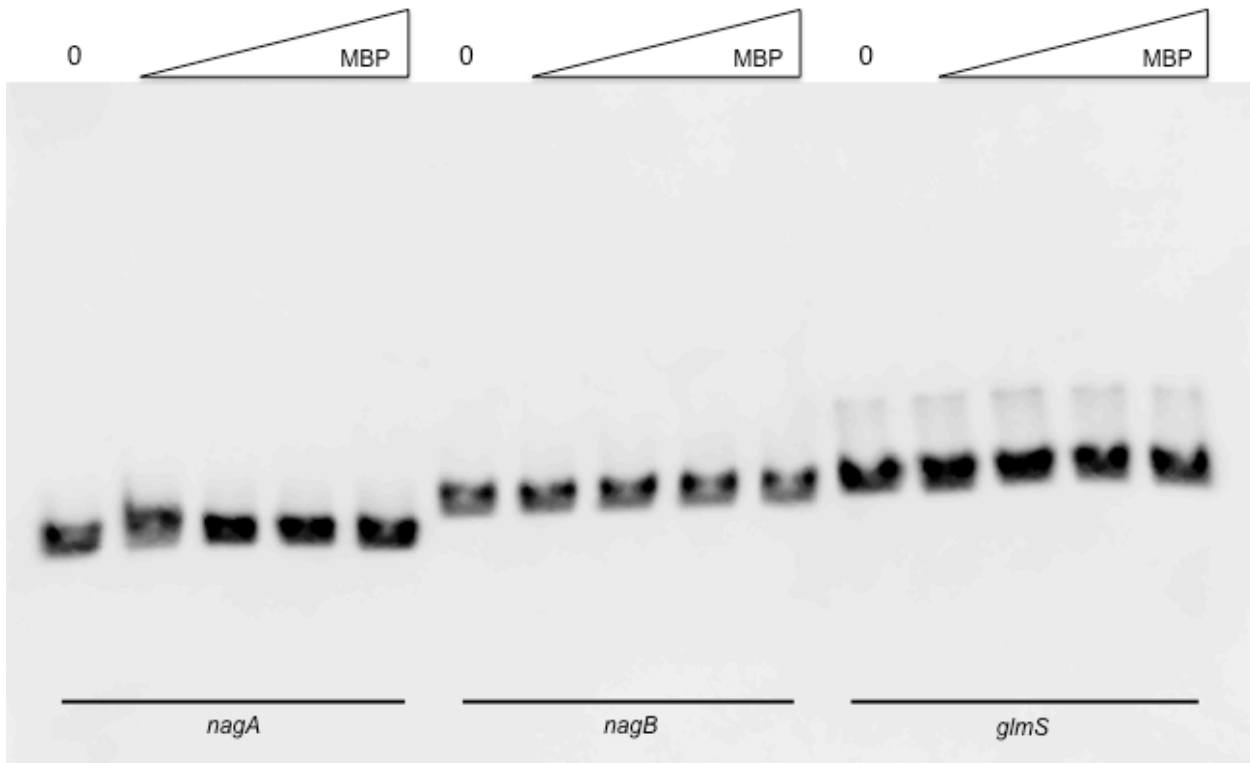


FIG S13 EMSA performed using increasing concentrations of the MBP-NagR (0-0.5 μM) fusion protein or the NagR released protein (0-4 μM) and biotinylated DNA containing the region upstream of the *nImD* (SMU.423; P384) or *pdhD* (SMU.1424; P1299) gene. EMSA is a representative example of at least three independent experiments showing similar results.

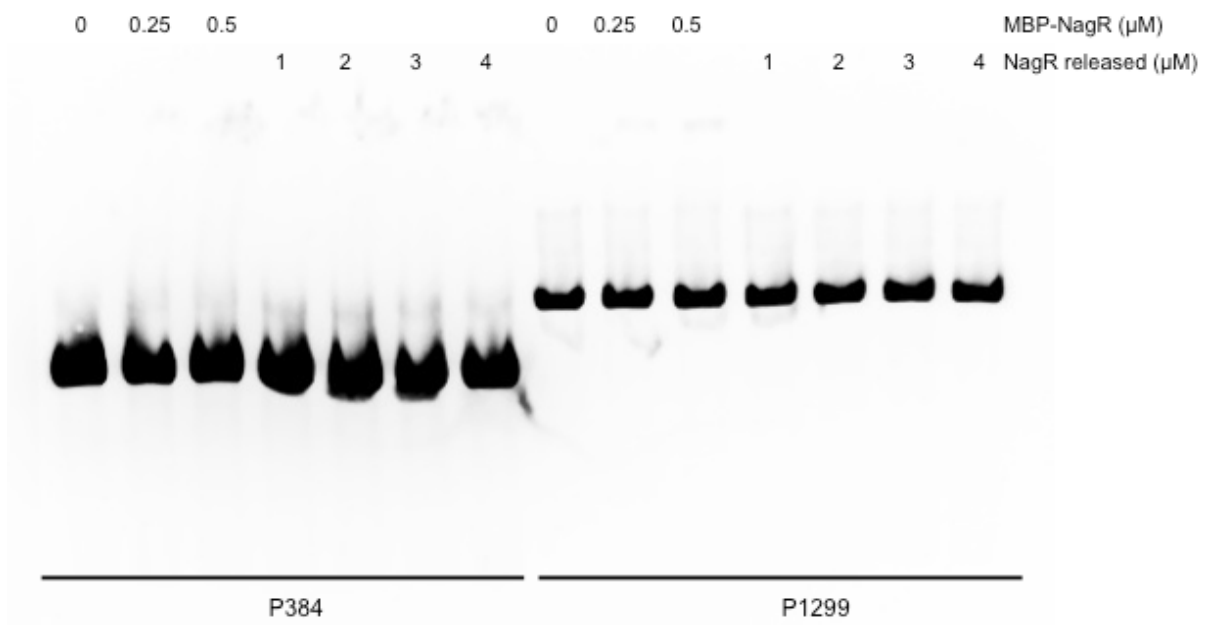


FIG S14 EMSA performed using a biotinylated fragment (10 fmol/reaction) of DNA corresponding to the region upstream of the *nagB* gene and increasing concentrations of NagR (0-1 μ M) protein. The non-ionic detergent NP-40 was added to reaction mixtures in order to discourage protein aggregation as described in the Materials and Methods section. At least three independent experiments were performed with each showing similar results.

